

Tunable anisotropic quantum Rabi model via magnon|spin-qubit ensemble

Ida C. Skogvoll,¹ Jonas Lidal,¹ Jeroen Danon,¹ and Akashdeep Kamra^{2,1,*}

¹*Center for Quantum Spintronics, Department of Physics,*

Norwegian University of Science and Technology, NO-7491 Trondheim, Norway

²*Condensed Matter Physics Center (IFIMAC) and Departamento de Física Teórica de la Materia Condensada, Universidad Autónoma de Madrid, E-28049 Madrid, Spain*

The ongoing rapid progress towards quantum technologies relies on and strives for new hybrid platforms optimized for specific quantum computation and communication tasks. We theoretically study a spin qubit exchange-coupled to an anisotropic ferromagnet that hosts magnons with a controllable degree of intrinsic squeezing. We find this system to physically realize the quantum Rabi model from isotropic to the Jaynes-Cummings limit with coupling strengths that can foray into the deep-strong regime. We demonstrate that the composite nature of the squeezed-magnon enables concurrent excitation of 3 spin qubits coupled to the same magnet. Thus, 3-qubit Greenberger-Horne-Zeilinger and related states needed for implementing Shor's quantum error correction code can be robustly generated. Our analysis highlights some unique advantages offered by this hybrid platform and hopes to motivate corresponding experimental efforts.

Introduction.—A bosonic mode interacting with a two-level system constitutes the paradigmatic quantum Rabi model (QRM) employed in understanding light-matter interaction [1, 2]. The recent theoretical discovery of its integrability [3] and increasing coupling strengths realized in experiments have brought the QRM into a sharp focus [4, 5]. It also models a qubit interacting with an electromagnetic mode, a key ingredient for quantum communication and distant qubit-qubit coupling [6–9]. Thus, the ongoing quantum information revolution [6, 10] capitalizes heavily on the advancements in physically realizing and theoretically understanding the QRM. In particular, larger coupling strengths are advantageous for faster gate operations on qubits, racing against imminent decoherence. Generating squeezed states of the bosonic mode [11, 12], typically light, via parametric amplification has emerged as a nonequilibrium means of strengthening this coupling [13, 14]. Other related methods [15, 16] that exploit drives to control, for example, the QRM anisotropy [4] have also been proposed.

Contemporary digital electronics relies heavily on the very-large-scale integration of the same silicon-based circuits. In sharp contrast, emerging quantum information technologies benefit from multiple physical realizations of qubits and their interconnects in order to choose the best platform for implementing a specific task or computation [6, 8, 17–20]. Fault-tolerant quantum computing, either via less error-prone qubits [21] or via implementation of quantum error correction [22–24], is widely seen as the path forward. A paradigmatic error correction code [22] put forth by Shor requires encoding one logical qubit into 9 physical qubits and generating 3-qubit Greenberger-Horne-Zeilinger (GHZ) [25] and related states. A continuous-variable analog of this code employing squeezed states of light has been experimentally demonstrated [26]. This has spurred fresh hopes of fault-tolerant quantum computing and demonstrated the bosonic modes as more than just interconnects for

qubits.

In our discussion above, we have encountered squeezed states of light in multiple contexts. These nonequilibrium states, bearing widespread applications from metrology [27] to quantum teleportation [28, 29], decay with time. In contrast, the bosonic normal modes - magnons - in anisotropic ferromagnets were recently shown to be squeezed [30] and embody various quantum features inherent to such squeezed states [11, 31–33]. Being equilibrium in nature, these are also somewhat different from light and require care when making comparisons. This calls for examining ways in which we can exploit the robust equilibrium-squeezed nature of magnons in addressing challenges facing emerging quantum technologies [20, 34, 35]. The spin qubit [18, 19, 36] becomes the perfect partner because of its potential silicon-based nature, feasibility of a strong exchange-coupling to the magnet, reliance on a mature fabrication technology and so on.

Here, we theoretically study a ferromagnet exchange-coupled to a spin qubit. We find the ensuing magnon|qubit ensemble to combine various complementary advantages mentioned above into one promising platform. We show that this system realizes an ideal Jaynes-Cummings model, enabled by spin conservation in the system that forbids the counter rotating terms (CRTs) by symmetry. Allowing anisotropy in the magnet, the squeezed-magnon [30, 31] becomes the normal mode giving rise to nonzero and controllable CRTs. The squeezed nature of the magnon further leads to an enhancement in the coupling strength, without the need for a nonequilibrium drive. Considering three spin qubits coupled to the same ferromagnet, we theoretically demonstrate the simultaneous and resonant excitation of the three qubits via a single squeezed-magnon. Thus, the system enables a robust means to generate the entangled 3-qubit GHZ and related states that underlie Shor's error correction code [22]. The magnon-spin qubit ensemble

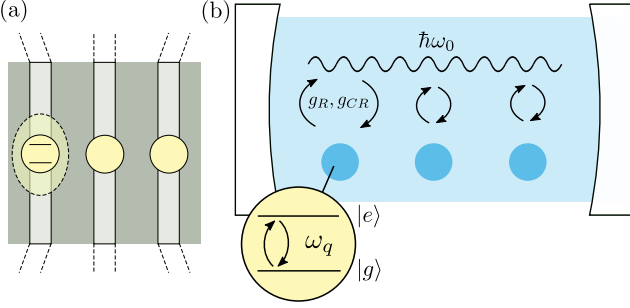


FIG. 1. Schematic depiction of 3 spin qubits exchange-coupled to 1 magnon mode. (a) Semiconducting wires hosting the localized electronic states that constitute the spin qubit are deposited on top of a thin insulating ferromagnet layer. A direct contact enables strong interfacial exchange coupling. (b) The corresponding anisotropic QRM. Three qubits interact with a single magnonic mode via controllably strong rotating (g_R) and counter-rotating (g_{CR}) terms [Eq. (9)].

offers an optimal platform for realizing the QRM with large coupling strengths and implementing fault-tolerant quantum computing protocols.

1 magnonic mode coupled to 1 qubit.—We consider a thin film of an insulating ferromagnet that acts as a magnonic cavity. Considering an applied magnetic field $H_0\hat{\mathbf{z}}$, the ferromagnetic Hamiltonian is expressed as [37]:

$$\tilde{H}_F = -J \sum_{\langle i,j \rangle} \tilde{\mathbf{S}}_i \cdot \tilde{\mathbf{S}}_j + |\gamma| \mu_0 H_0 \sum_i \tilde{S}_{iz}, \quad (1)$$

where J (> 0) parametrizes ferromagnetic exchange between the nearest neighbors, γ (< 0) is the gyromagnetic ratio, and $\tilde{\mathbf{S}}_i$ denotes the spin operator at position i . We set $\hbar = 1$ throughout and identify operators with an overhead tilde. A detailed derivation of the system Hamiltonian is presented in the Supplemental Material (SM) [38]. In its ground state, the ferromagnet has all its spins pointing along $-\hat{\mathbf{z}}$. Employing Holstein-Primakoff transformations [39] and switching to Fourier space, the ferromagnetic Hamiltonian is written in terms of spin-1 magnons [38]:

$$\tilde{H}_F = \text{const.} + \sum_{\mathbf{k}} (\omega_0 + c_l J S a^2 k^2) \tilde{a}_{\mathbf{k}}^\dagger \tilde{a}_{\mathbf{k}}, \quad (2)$$

where $\omega_0 \equiv |\gamma| \mu_0 H_0$ is the ferromagnetic resonance frequency (\sim GHz) corresponding to the uniform ($\mathbf{k} = \mathbf{0}$) magnon mode, a is the lattice constant, S is the spin, c_l is a factor that depends on the considered lattice, $\tilde{a}_{\mathbf{k}}$ denotes the annihilation operator for a magnon with wavevector \mathbf{k} . The boundary conditions for small magnets result in a discrete magnon spectrum [40]. For typical values of J , spatial dimensions in the μm range result in the magnon energies differing by a few GHz. Hence, we consider only the $\mathbf{k} = \mathbf{0}$ mode henceforth, denoting \tilde{a}_0

simply as \tilde{a} . We may disregard the higher modes as we exploit coherent resonant interactions in this study.

As depicted in Fig. 1(a), the confined electron gas that becomes a spin qubit is interfaced directly with the ferromagnet to enable exchange-coupling [41–44]:

$$\tilde{H}_{\text{int}} = J_{\text{int}} \sum_l \tilde{\mathbf{S}}_l \cdot \tilde{\mathbf{s}}_l, \quad (3)$$

where J_{int} parameterizes the interfacial exchange interaction, $\tilde{\mathbf{s}}_l$ denotes the spin operator of the spin qubit electronic state at site l , and l runs over the interfacial sites. In terms of the relevant eigenmodes, the interfacial interaction is simplified as [38]:

$$\tilde{H}_{\text{int}} = g (\tilde{a}^\dagger \tilde{\sigma}_- + \tilde{a} \tilde{\sigma}_+), \quad (4)$$

where $g = J_{\text{int}} N_{\text{int}} |\psi|^2 \sqrt{S/(2N_F)}$, with N_{int} the number of interfacial sites, $|\psi|^2$ the spin qubit electron probability averaged over the interface [38], and N_F the total number of sites in the ferromagnet. $\tilde{\sigma}_{+,-} = (\tilde{\sigma}_x \pm i\tilde{\sigma}_y)/2$ excite or relax the spin qubit that is further described via:

$$\tilde{H}_q = \frac{\omega_q}{2} \tilde{\sigma}_z. \quad (5)$$

Thus, our total Hamiltonian becomes

$$\tilde{H}_1 = \tilde{H}_F + \tilde{H}_q + \tilde{H}_{\text{int}}, \quad (6)$$

where $\tilde{H}_F = \omega_0 \tilde{a}^\dagger \tilde{a}$ and the other contributions are given by Eqs. (4) and (5).

Our system thus realizes the Jaynes-Cummings Hamiltonian [Eq. (6)] that conserves the total number of excitations. This is a direct consequence of spin conservation afforded by the exchange-coupling in our system. A spin-1 magnon can be absorbed by a spin qubit flipping the latter from its spin $-1/2$ to $+1/2$ state. The same transition in the spin qubit, however, cannot emit a magnon. This is in contrast with the case of dipolar coupling between the spin qubit and the ferromagnet [7, 37, 44–46], which does not necessarily conserve spin. Further, as numerically estimated below, on account of exchange being a much stronger interaction, the effective coupling g in our system can exceed the magnon frequency ω_0 thereby covering the full coupling range from weak to deep-strong [47–49]. Nonclassical behavior is typically manifested starting with ultrastrong couplings $g/\omega_0 > 0.1$ [47, 50, 51].

We have considered the ferromagnet to be isotropic thus far. However, such films manifest a strong shape anisotropy, in addition to potential magnetocrystalline anisotropies [37]. We now include such effects by adding the following term to the ferromagnet Hamiltonian:

$$\tilde{H}_{\text{an}} = \sum_i K_x (\tilde{S}_{ix})^2 + K_y (\tilde{S}_{iy})^2 + K_z (\tilde{S}_{iz})^2,$$

which results in the following magnon Hamiltonian, retaining only the uniform mode:

$$\tilde{H}_F = A\tilde{a}^\dagger\tilde{a} + B(\tilde{a}^2 + \tilde{a}^{\dagger 2}), \quad (7)$$

with $A \equiv |\gamma|\mu_0H_0 + K_xS + K_yS - 2K_zS$ and $B \equiv S(K_x - K_y)/2$. The ensuing Hamiltonian possesses the squeezing terms $\propto B$ which, unlike in the case of light, result from the magnet trying to minimize its ground state energy while respecting the Heisenberg uncertainty principle [31]. The new eigenmode, dubbed squeezed-magnon [30], is obtained via a Bogoliubov transform $\tilde{a} = \cosh r\tilde{\alpha} + \sinh r\tilde{\alpha}^\dagger$ resulting in

$$\tilde{H}_F = \omega_0\tilde{\alpha}^\dagger\tilde{\alpha}, \quad (8)$$

where we continue to denote the eigenmode energy as ω_0 , which now becomes $\omega_0 = \sqrt{A^2 - 4B^2}$. Further, the squeeze parameter r is governed by the relation $\sinh r = -2B/\sqrt{(A + \omega_0)^2 - 4B^2}$ [52]. In the new eigenbasis, we obtain:

$$\tilde{H}_{\text{int}} = g_R(\tilde{\alpha}^\dagger\tilde{\sigma}_- + \tilde{\alpha}\tilde{\sigma}_+) + g_{CR}(\tilde{\alpha}^\dagger\tilde{\sigma}_+ + \tilde{\alpha}\tilde{\sigma}_-), \quad (9)$$

with $g_R = g \cosh r$ and $g_{CR} = g \sinh r$. The interaction now bears both rotating ($\propto g_R$) and counter-rotating ($\propto g_{CR}$) terms [Fig. 1(b)].

Our system can be analyzed in terms of two different bases: using spin-1 magnon (represented by \tilde{a}) or squeezed-magnon ($\tilde{\alpha}$). The latter is the eigenmode and is comprised of a superposition of odd magnon-number states [Fig. 2(a)] [30, 31, 53, 54]. Since a spin-1 magnon is associated with the physical spin-flip in the magnet [39], the interaction Eq. (4) is still comprised of absorption and emission of magnons (\tilde{a}) accompanied by transitions in the qubit. On the other hand, in the eigenbasis, the qubit is now interacting with a new bosonic eigenmode - the squeezed-magnon ($\tilde{\alpha}$) via an interaction bearing rotating and CRTs [Eq. (9)]. Therefore, in the eigenbasis, our system accomplishes an anisotropic QRM [4, 5] [Fig. 1(b)] - Eqs. (5), (6), (8), and (9). The squeeze parameter r , tunable via applied field and anisotropies [55], further enhances the coupling strength and controls the relative importance of the rotating and CRTs: $g_R = g \cosh r$ and $g_{CR} = g \sinh r$.

1 magnonic mode coupled to 3 qubits.—We now exploit the squeezed and composite nature of the magnonic eigenmode in generating useful entangled states [31]. As depicted in Fig. 2(a), the composite nature of the squeezed-magnon should enable joint excitation of an odd number of qubits. Considering the paramount importance of generating such 3-qubit GHZ states [25] for Shor's error correction code [22], we consider 3 qubits coupled to the same squeezed-magnon eigenmode:

$$\tilde{H}_3 = \tilde{H}_F + \sum_{n=1,2,3} (\tilde{H}_q^n + \tilde{H}_{\text{int}}^n), \quad (10)$$

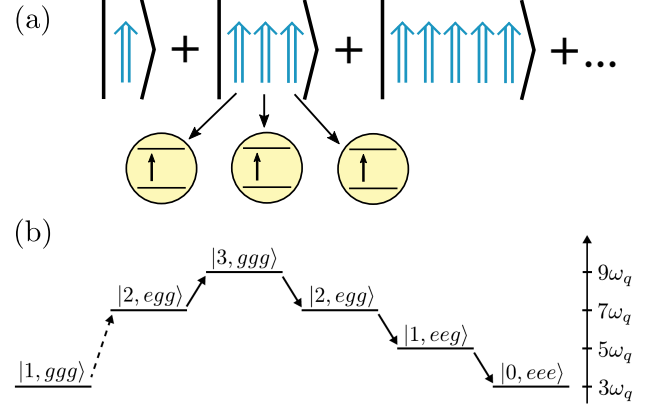


FIG. 2. Schematic depiction of the transition $|1, ggg\rangle \rightarrow |0, eee\rangle$. (a) The squeezed-magnon is comprised of a superposition of odd magnon-number states. This composite nature enables its absorption by an odd number of qubits. We focus on the case of 3. (b) An example pathway that takes the system from bearing 1 squeezed-magnon and 3 ground-state qubits ($|1, ggg\rangle$) to 0 squeezed-magnon and 3 excited qubits ($|0, eee\rangle$) via a series of virtual states. The first transition is effected by a CRT and is indicated via a dashed arrow. The right scale indicates the state energy, assuming $\omega_0 = 3\omega_q$.

with individual contributions expressed via Eqs. (5), (8), and (9). For simplicity, we assume the three qubits and their coupling with the magnet to be identical. The qualitative physics is unaffected by asymmetries among the 3 qubits, which are detailed in the SM [38]. Henceforth, we analyze the problem in its eigenbasis employing methodology consistent with previous investigation of joint photon absorption [56].

We are interested in jointly exciting the three qubits using a single squeezed-magnon eigenmode: a transition denoted as $|1, ggg\rangle \rightarrow |0, eee\rangle$. To gain physical insight, we first analyze this transition within the perturbation-theory framework detailed in the SM [38, 57]. While the transition is not possible via a direct process [first order in the interaction Eq. (9)], it can be accomplished via a series of virtual processes. As the transition requires an increase of the total excitation number by 2, at least one of the virtual processes should be effected via the CRTs, thus requiring nonzero squeezing r in our system. The shortest path to effect the transition consists of three virtual processes, but its amplitude is canceled exactly by a complementary path [38]. Hence, the lowest nonvanishing order for accomplishing this transition is five with an example pathway depicted in Fig. 2(b) [58]. As detailed in the SM [38], several such paths contribute to the overall transition amplitude. The energy conservation requirement on the initial and final states necessitates $\omega_0 \approx 3\omega_q$.

Guided by intuition from the perturbative analysis, we now study the system [Eq. (10)] numerically using the

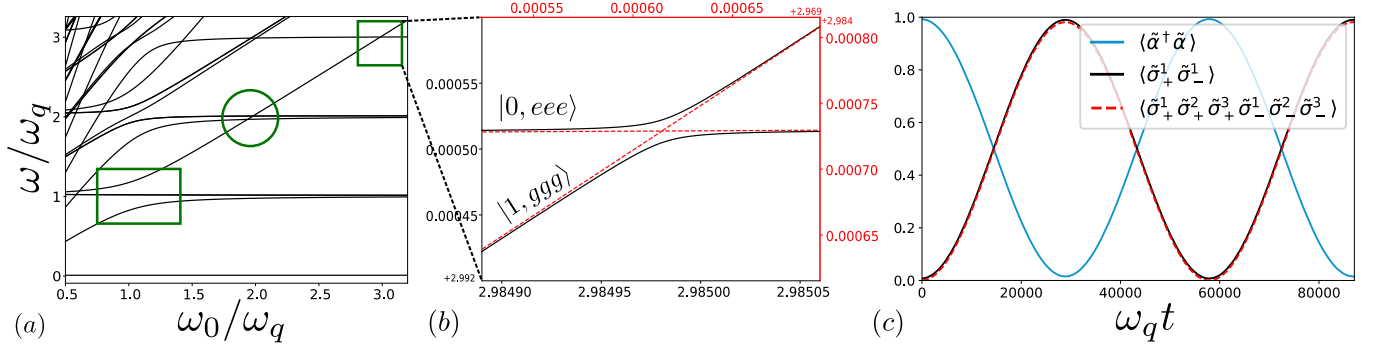


FIG. 3. Numerically evaluated spectrum and dynamics of 3 qubits coupled to 1 magnonic mode [Eq. (10)]. (a) Energy spectrum evaluated assuming $g_R = g_{CR} = 0.1\omega_q$. The green rectangle encloses the typical one-excitation anticrossing ($\omega_0 \approx \omega_q$). The circle highlights crossings around $\omega_0 \approx 2\omega_q$ as only odd number of qubits can be excited [Fig. 2(a)]. The square emphasizes the weaker three-excitation anticrossing around $\omega_0 \approx 3\omega_q$ that results from finite squeezing and the resulting CRTs. (b) A zoom-in on the three-excitation anticrossing that stems from the transition depicted in Fig. 2. The red dashed lines depict the spectrum evaluated assuming $g_{CR} = 0$ leaving the rest unchanged. (c) Zero-detuning system dynamics around $\omega_0 \approx 3\omega_q$ with the initial state $|1,ggg\rangle$. The squeezed-magnon occupation (blue solid) and single-qubit excitation (black solid) manifest the typical Rabi oscillations. A nearly perfect overlap between single-qubit and three-qubit (red dashed) correlations confirms the joint nature of the three-qubit excitation in these Rabi oscillations.

QuTiP package [59, 60]. Unless stated otherwise, we employ $g_R = g_{CR} = 0.1\omega_q$ in our analysis. A numerical diagonalization of the total Hamiltonian Eq. (10) yields the energy spectrum as depicted in Fig. 3(a). For zero qubit-magnon coupling, the spectrum should contain 8 (2^3) flat curves corresponding to the different excited qubits and zero squeezed-magnon occupation. Two triplets of these overlap resulting in 4 visually-distinct flat curves. The same 3-qubit spectrum combined with N squeezed-magnons yields the same 4 visually-distinct curves, now with a slope of N . For small but finite coupling considered in Fig. 3(a), we see the typical one-excitation Rabi splitting around $\omega_0 \approx \omega_q$ that results from a direct process. Around $\omega_0 \approx 2\omega_q$, we see crossings between different levels [61]. A coupling here is forbidden as only odd number of qubits can be excited by one squeezed-magnon [Fig. 2(a)]. An apparent crossing around $\omega_0 \approx 3\omega_q$ is in fact an anticrossing manifesting a small Rabi splitting between the states $|1,ggg\rangle$ and $|0,eee\rangle$ [see Fig. 3(b)]. This is the transition of our interest and the effective coupling responsible for it can be expressed as:

$$\tilde{H}_{\text{eff}} = g_{\text{eff}} (|1,ggg\rangle \langle 0,eee| + |0,eee\rangle \langle 1,ggg|), \quad (11)$$

where $g_{\text{eff}}/\omega_q = 0.0001(g_{CR}/\omega_q) - 0.003(g_{CR}/\omega_q)^3$ has been obtained by fitting (perfectly) its g_{CR} dependence predicted by the perturbative analysis [38] to the Rabi splittings obtained via numerical diagonalization [62]. A comparison between squeezed-magnon occupation, single-qubit excitation, and three-qubit correlations plotted in Fig. 3(c) for Rabi oscillations around $\omega_0 \approx 3\omega_q$ confirms the joint nature of the three-qubit excitation.

Discussion.—Our system enables the transition $|1,ggg\rangle \rightarrow |0,eee\rangle$ with an effective coupling strength

g_{eff} [Eq. (11)], or equivalently Rabi frequency, tunable via the magnon-squeezing: $g_{CR} = g \sinh r$. Bringing the system in resonance to enable Rabi oscillation for a fraction of the cycle can be exploited in generating 3-qubit GHZ and related entangled states: $(|ggg\rangle \pm |eee\rangle)/\sqrt{2}$. A convenient generation of these is central to Shor's error correction code [22] and thus, of great value in achieving fault tolerant quantum computing. Generating such 3-qubit entangled states using a series of two-qubit gate operations inevitably suffers from the challenge of synchronizing exact pulses, qubit asymmetries, decoherence and so on. In contrast, capitalizing on energy conservation, our proposed method is robust against any qubit asymmetries and perfectly synchronizes excitation of the 3 qubits.

Being a fifth-order process, g_{eff} was evaluated to be small for the parameters employed in our analysis above ($g_R = g_{CR} = 0.1\omega_q$). However, notwithstanding our choice of parameters motivated by a comparison with perturbation theory, the proposed system can achieve very high bare couplings g [Eq. (9)] ($g_R, g_{CR} > \omega_q$), such that the higher-order processes are not diminished and g_{eff} becomes large. Spin pumping experiments yield interfacial exchange couplings [Eq. (3)] of $J_{\text{int}} \approx 10$ meV between various (insulating) magnets and adjacent metals [63–65]. Assuming the qubit wavefunction to be localized in 5 monolayers below the equally thin ferromagnet and an interface comprised of 100 sites, we obtain the bare coupling rate [Eq. (4)] $g \approx 0.005J_{\text{int}} \approx 80$ GHz, significantly larger than typical spin qubit and uniform magnon mode frequencies.

Our proposal of leveraging the intrinsic magnon-squeezing in generating entanglement via a coherent pro-

cess is complementary to previous incoherent interaction-based proposals [32, 44, 66, 67]. The latter typically necessitate diabatic decoupling of qubits from the magnet after achieving an entangled state. Our proposal thus uncovers an unexplored and experimentally-favorable avenue for exploiting the squeezing intrinsic to magnets.

Summary.—We have demonstrated the magnon|spin qubit ensemble to realize the anisotropic quantum Rabi model with coupling strengths feasible in the deep-strong regime. This system is shown to capitalize on various unique features of squeezed-magnons hosted by magnets. These include squeezing-mediated coupling enhancement, tunable anisotropy of the Rabi model, and a convenient synchronous entanglement of 3 qubits. Thus, the magnon|spin qubit ensemble provides a promising platform for investigating phenomena beyond the ultrastrong regime and implementing error correction codes.

We thank Wolfgang Belzig, Tim Ludwig, and Rembert Duine for valuable discussions. We acknowledge financial support from the Research Council of Norway through its Centers of Excellence funding scheme, project 262633, “QuSpin”, and the Spanish Ministry for Science and Innovation – AEI Grant CEX2018-000805-M (through the “Maria de Maeztu” Programme for Units of Excellence in R&D).

* akashdeep.kamra@uam.es

- [1] I. I. Rabi, “On the process of space quantization,” *Phys. Rev.* **49**, 324–328 (1936).
- [2] I. I. Rabi, “Space quantization in a gyrating magnetic field,” *Phys. Rev.* **51**, 652–654 (1937).
- [3] D. Braak, “Integrability of the rabi model,” *Phys. Rev. Lett.* **107**, 100401 (2011).
- [4] Qiong-Tao Xie, Shuai Cui, Jun-Peng Cao, Luigi Amico, and Heng Fan, “Anisotropic rabi model,” *Phys. Rev. X* **4**, 021046 (2014).
- [5] Qiongtao Xie, Honghua Zhong, Murray T Batchelor, and Chaohong Lee, “The quantum rabi model: solution and dynamics,” *Journal of Physics A: Mathematical and Theoretical* **50**, 113001 (2017).
- [6] Stephanie Wehner, David Elkouss, and Ronald Hanson, “Quantum internet: A vision for the road ahead,” *Science* **362** (2018), 10.1126/science.aam9288.
- [7] Masaya Fukami, Denis R. Candido, David D. Awschalom, and Michael E. Flatté, “Opportunities for long-range magnon-mediated entanglement of spin qubits via on- and off-resonant coupling,” (2021), arXiv:2101.09220 [quant-ph].
- [8] D. D. Awschalom, C. H. R. Du, R. He, F. J. Heremans, A. Hoffmann, J. T. Hou, H. Kurebayashi, Y. Li, L. Liu, V. Novosad, J. Sklenar, S. E. Sullivan, D. Sun, H. Tang, V. Tiberkevich, C. Trevillian, A. W. Tsien, L. R. Weiss, W. Zhang, X. Zhang, L. Zhao, and C. W. Zolitsch, “Quantum engineering with hybrid magnonics systems and materials,” (2021), arXiv:2102.03222 [cond-mat.mes-hall].
- [9] Guido Burkard, Michael J. Gullans, Xiao Mi, and Jason R. Petta, “Superconductor–semiconductor hybrid-circuit quantum electrodynamics,” *Nat. Rev. Phys.* **2**, 129–140 (2020), 1905.01155.
- [10] Arne Laucht, Frank Hohls, Niels Ubbelohde, M Fernando Gonzalez-Zalba, David J Reilly, Sren Stobbe, Tim Schrder, Pasquale Scarlino, Jonne V Koski, Andrew Dzurak, Chih-Hwan Yang, Jun Yoneda, Ferdinand Kuemmeth, Hendrik Bluhm, Jarryd Pla, Charles Hill, Joe Salfi, Akira Oiwa, Juha T Muhonen, Ewold Verhagen, M D LaHaye, Hyun Ho Kim, Adam W Tsien, Dimitrie Culcer, Attila Geresdi, Jan A Mol, Varun Mohan, Prashant K Jain, and Jonathan Baugh, “Roadmap on quantum nanotechnologies,” *Nanotechnology* **32**, 162003 (2021), 2101.07882.
- [11] C. Gerry and P. Knight, *Introductory Quantum Optics* (Cambridge University Press, 2004).
- [12] D. F. Walls, “Squeezed states of light,” *Nature* **306**, 141 (1983).
- [13] Wei Qin, Adam Miranowicz, Peng-Bo Li, Xin-You Lü, J. Q. You, and Franco Nori, “Exponentially enhanced light-matter interaction, cooperativities, and steady-state entanglement using parametric amplification,” *Phys. Rev. Lett.* **120**, 093601 (2018).
- [14] C. Leroux, L. C. G. Govia, and A. A. Clerk, “Enhancing cavity quantum electrodynamics via antisqueezing: Synthetic ultrastrong coupling,” *Phys. Rev. Lett.* **120**, 093602 (2018).
- [15] Gangcheng Wang, Ruoqi Xiao, H. Z. Shen, Chunfang Sun, and Kang Xue, “Simulating anisotropic quantum rabi model via frequency modulation,” *Scientific Reports* **9**, 4569 (2019).
- [16] Carlos Sánchez Muñoz, Anton Frisk Kockum, Adam Miranowicz, and Franco Nori, “Simulating ultrastrong-coupling processes breaking parity conservation in jaynes-cummings systems,” *Phys. Rev. A* **102**, 033716 (2020).
- [17] Maximilian Russ and Guido Burkard, “Three-electron spin qubits,” *Journal of Physics: Condensed Matter* **29**, 393001 (2017).
- [18] Anasua Chatterjee, Paul Stevenson, Silvano De Franceschi, Andrea Morello, Nathalie P. de Leon, and Ferdinand Kuemmeth, “Semiconductor qubits in practice,” *Nature Reviews Physics* **3**, 157–177 (2021), 2005.06564.
- [19] Lieven M. K. Vandersypen and Mark A. Eriksson, “Quantum computing with semiconductor spins,” *Physics Today* **72**, 38–45 (2019).
- [20] Dany Lachance-Quirion, Yutaka Tabuchi, Arnaud Gloppe, Koji Usami, and Yasunobu Nakamura, “Hybrid quantum systems based on magnonics,” *Applied Physics Express* **12**, 070101 (2019).
- [21] Chetan Nayak, Steven H. Simon, Ady Stern, Michael Freedman, and Sankar Das Sarma, “Non-abelian anyons and topological quantum computation,” *Rev. Mod. Phys.* **80**, 1083–1159 (2008).
- [22] Peter W. Shor, “Scheme for reducing decoherence in quantum computer memory,” *Phys. Rev. A* **52**, R2493–R2496 (1995).
- [23] B M Terhal, J Conrad, and C Vuillot, “Towards scalable bosonic quantum error correction,” *Quantum Science and Technology* **5**, 043001 (2020).
- [24] Daniel Gottesman, Alexei Kitaev, and John Preskill, “Encoding a qubit in an oscillator,” *Physical Review A* **64**, 012310 (2001).

[25] Daniel M. Greenberger, Michael A. Horne, and Anton Zeilinger, “Going beyond bell’s theorem,” (2007), arXiv:0712.0921 [quant-ph].

[26] Takao Aoki, Go Takahashi, Tadashi Kajiya, Jun-ichi Yoshikawa, Samuel L. Braunstein, Peter van Loock, and Akira Furusawa, “Quantum error correction beyond qubits,” *Nature Physics* **5**, 541 (2009).

[27] Roman Schnabel, “Squeezed states of light and their applications in laser interferometers,” *Physics Reports* **684**, 1 – 51 (2017).

[28] Z. Y. Ou, S. F. Pereira, H. J. Kimble, and K. C. Peng, “Realization of the einstein-podolsky-rosen paradox for continuous variables,” *Phys. Rev. Lett.* **68**, 3663–3666 (1992).

[29] G. J. Milburn and Samuel L. Braunstein, “Quantum teleportation with squeezed vacuum states,” *Phys. Rev. A* **60**, 937–942 (1999).

[30] Akashdeep Kamra and Wolfgang Belzig, “Superpoissonian shot noise of squeezed-magnon mediated spin transport,” *Phys. Rev. Lett.* **116**, 146601 (2016).

[31] Akashdeep Kamra, Wolfgang Belzig, and Arne Brataas, “Magnon-squeezing as a niche of quantum magnonics,” *Applied Physics Letters* **117**, 090501 (2020).

[32] Ji Zou, Se Kwon Kim, and Yaroslav Tserkovnyak, “Tuning entanglement by squeezing magnons in anisotropic magnets,” *Phys. Rev. B* **101**, 014416 (2020).

[33] Sanchar Sharma, Victor A. S. V. Bittencourt, Alexy D. Karenowska, and Silvia Viola Kusminskiy, “Spin cat states in ferromagnetic insulators,” *Phys. Rev. B* **103**, L100403 (2021).

[34] Yi-Pu Wang and Can-Ming Hu, “Dissipative couplings in cavity magnonics,” *Journal of Applied Physics* **127**, 130901 (2020).

[35] Yutaka Tabuchi, Seiichiro Ishino, Atsushi Noguchi, Toyofumi Ishikawa, Rekishi Yamazaki, Koji Usami, and Yasunobu Nakamura, “Coherent coupling between a ferromagnetic magnon and a superconducting qubit,” *Science* **349**, 405–408 (2015).

[36] Daniel Loss and David P. DiVincenzo, “Quantum computation with quantum dots,” *Phys. Rev. A* **57**, 120–126 (1998).

[37] A.I. Akhiezer, V.G. Bar’iakhtar, and S.V. Peletminski, *Spin waves* (North-Holland Publishing Company, Amsterdam, 1968).

[38] See Supplemental Material for (i) a detailed derivation of the system Hamiltonian and (ii) a detailed perturbation-theory based analysis of the simultaneous three-qubit excitation including the various third-order and fifth-order virtual processes as well as the resilience of the phenomena against qubit-asymmetries.

[39] T. Holstein and H. Primakoff, “Field dependence of the intrinsic domain magnetization of a ferromagnet,” *Phys. Rev.* **58**, 1098–1113 (1940).

[40] Daniel D. Stancil and Anil Prabhakar, *Spin Waves: Theory and Applications* (Springer US, 2009).

[41] S. Takahashi, E. Saitoh, and S. Maekawa, “Spin current through a normal-metal/insulating-ferromagnet junction,” *Journal of Physics: Conference Series* **200**, 062030 (2010).

[42] Scott A. Bender and Yaroslav Tserkovnyak, “Interfacial spin and heat transfer between metals and magnetic insulators,” *Phys. Rev. B* **91**, 140402 (2015).

[43] Akashdeep Kamra and Wolfgang Belzig, “Magnon-mediated spin current noise in ferromagnet | nonmagnetic conductor hybrids,” *Phys. Rev. B* **94**, 014419 (2016).

[44] Luka Trifunovic, Fabio L. Pedrocchi, and Daniel Loss, “Long-distance entanglement of spin qubits via ferromagnet,” *Phys. Rev. X* **3**, 041023 (2013).

[45] B. Flebus and Y. Tserkovnyak, “Quantum-impurity relaxometry of magnetization dynamics,” *Phys. Rev. Lett.* **121**, 187204 (2018).

[46] Chunhui Du, Toeno van der Sar, Tony X. Zhou, Pramey Upadhyaya, Francesco Casola, Huiliang Zhang, Mehmet C. Onbasli, Caroline A. Ross, Ronald L. Walsworth, Yaroslav Tserkovnyak, and Amir Yacoby, “Control and local measurement of the spin chemical potential in a magnetic insulator,” *Science* **357**, 195–198 (2017).

[47] Anton Frisk Kockum, Adam Miranowicz, Vincenzo Macrì, Salvatore Savasta, and Franco Nori, “Deterministic quantum nonlinear optics with single atoms and virtual photons,” *Phys. Rev. A* **95**, 063849 (2017).

[48] J. Casanova, G. Romero, I. Lizuain, J. J. García-Ripoll, and E. Solano, “Deep strong coupling regime of the jaynes-cummings model,” *Phys. Rev. Lett.* **105**, 263603 (2010).

[49] T. Niemczyk, F. Deppe, H. Huebl, E. P. Menzel, F. Hocke, M. J. Schwarz, J. J. García-Ripoll, D. Zueco, T. Hümmer, E. Solano, A. Marx, and R. Gross, “Circuit quantum electrodynamics in the ultrastrong-coupling regime,” *Nature Physics* **6**, 772 (2010).

[50] P. Forn-Díaz, L. Lamata, E. Rico, J. Kono, and E. Solano, “Ultrastrong coupling regimes of light-matter interaction,” *Rev. Mod. Phys.* **91**, 025005 (2019).

[51] S. Ashhab and Franco Nori, “Qubit-oscillator systems in the ultrastrong-coupling regime and their potential for preparing nonclassical states,” *Phys. Rev. A* **81**, 042311 (2010).

[52] The ground state stability ensures $\omega_0 > 0$ and $(A + \omega_0)^2 > 4B^2$.

[53] Michael Martin Nieto, “Displaced and squeezed number states,” *Physics Letters A* **229**, 135 – 143 (1997).

[54] P. Král, “Displaced and squeezed fock states,” *Journal of Modern Optics* **37**, 889–917 (1990).

[55] The magnetocrystalline anisotropies can be tuned via strain, for example.

[56] Luigi Garziano, Vincenzo Macrì, Roberto Stassi, Omar Di Stefano, Franco Nori, and Salvatore Savasta, “One Photon Can Simultaneously Excite Two or More Atoms,” *Phys. Rev. Lett.* **117**, 043601 (2016).

[57] W. R. Salzman, “Diagrammatical Derivation and Representation of Rayleigh–Schrödinger Perturbation Theory,” *The Journal of Chemical Physics* **49**, 3035–3040 (1968).

[58] Since this path involves 4 rotating and 1 counter-rotating processes, its amplitude scales as $\sim g_C R g_R^4$.

[59] J.R. Johansson, P.D. Nation, and Franco Nori, “Qutip: An open-source python framework for the dynamics of open quantum systems,” *Computer Physics Communications* **183**, 1760–1772 (2012).

[60] J.R. Johansson, P.D. Nation, and Franco Nori, “Qutip 2: A python framework for the dynamics of open quantum systems,” *Computer Physics Communications* **184**, 1234–1240 (2013).

[61] The nature “crossing”, as opposed to anticrossing, of these intersections has been verified carefully by evaluating the energy spectra around them with a very high precision.

[62] The reported g_{eff} has been obtained for $g_R = 0.1\omega_q$.

[63] Y. Kajiwara, K. Harii, S. Takahashi, J. Ohe, K. Uchida, M. Mizuguchi, H. Umezawa, H. Kawai, K. Ando, K. Takanashi, S. Maekawa, and E. Saitoh, “Transmission of electrical signals by spin-wave interconversion in a magnetic insulator,” *Nature* **464**, 262–266 (2010).

[64] F. D. Czeschka, L. Dreher, M. S. Brandt, M. Weiler, M. Althammer, I.-M. Imort, G. Reiss, A. Thomas, W. Schoch, W. Limmer, H. Huebl, R. Gross, and S. T. B. Goennenwein, “Scaling behavior of the spin pumping effect in ferromagnet-platinum bilayers,” *Phys. Rev. Lett.* **107**, 046601 (2011).

[65] Mathias Weiler, Matthias Althammer, Michael Schreier, Johannes Lotze, Matthias Pernpeintner, Sibylle Meyer, Hans Huebl, Rudolf Gross, Akashdeep Kamra, Jiang Xiao, Yan-Ting Chen, HuJun Jiao, Gerrit E. W. Bauer, and Sebastian T. B. Goennenwein, “Experimental test of the spin mixing interface conductivity concept,” *Phys. Rev. Lett.* **111**, 176601 (2013).

[66] Akashdeep Kamra, Even Thingstad, Gianluca Rastelli, Rembert A. Duine, Arne Brataas, Wolfgang Belzig, and Asle Sudbø, “Antiferromagnetic magnons as highly squeezed fock states underlying quantum correlations,” *Phys. Rev. B* **100**, 174407 (2019).

[67] H. Y. Yuan, Akashdeep Kamra, Dion M. F. Hartmann, and Rembert A. Duine, “Electrically switchable entanglement channel in van der waals magnets,” (2021), arXiv:2103.15899 [cond-mat.mes-hall].